Design of hard x-ray self-seeding monochromator for European XFEL

Cite as: AIP Conference Proceedings **2054**, 030016 (2019); https://doi.org/10.1063/1.5084579
Published Online: 16 January 2019

Liubov Samoylova, Deming Shu, Xiaohao Dong, et al.

Design of Hard X-Ray Self-Seeding Monochromator for European XFEL

Liubov Samoylova[1], Deming Shu[2], Xiaohao Dong[1], Gianluca Geloni[1], Suren Karabekyan[1], Sergey Terentev[3], Vladimir Blank[3], Shan Liu[4], Torsten Wohlenberg[4], Winfried Decking[4] and Harald Sinn[1]

[1]*European X-Ray Free-Electron Laser Facility, Holzkoppel 4, D-22869 Schenefeld, Germany.*
[2]*Argonne National Laboratory, Argonne II 60439, USA.*
[3]*Technological Institute for Superhard and Novel Carbon Materials, 142190 Moscow, Russia.*
[4]*Deutsches Elektronen-Synchrotron DESY, Notkestraße 85, 22607 Hamburg, Germany.*

[a)]Corresponding author: liubov.samoylova@xfel.eu

Abstract. Self-amplified spontaneous emission (SASE) XFELs are unique sources producing extremely powerful, ultra-short X-ray pulses. However, they rely on the amplification of the electron beam shot-noise, resulting in a relatively broad, spiky radiation spectrum. The poor temporal coherence of the SASE radiation is very unfavorable for many applications. A self-seeding scheme using X rays from the first part of the undulator to seed the second part, based on diamond single crystal monochromator, allows producing nearly Fourier-transform-limited X-ray pulses with the 1e-4 relative bandwidth at 9 keV. In our presentation, we will report on the main features of the custom designed monochromator system capable of handling the severe heat load coming from the high repetition rate of the FEL pulses (up to thousands pulses in trains with 10 Hz repetition rate) as well as the spontaneous radiation. High-quality synthetic diamonds used in the seeding monochromator combine high lattice perfection, low absorption of the x rays, very high heat conductivity and small thermal expansion. For deformation-free mounting of the diamond crystals to the holder, the crystal plates are manufactured in a special form with cuts that decouple the mechanical fixture part in the holder from the defect free working area. A hard X-ray self-seeding monochromator setup will be ready for installation at the SASE2 undulator beamline of the European XFEL soon, and its commissioning is planned for the beginning of 2019.

INTRODUCTION

For the European XFEL operating in the hard X-ray range, the typical X-ray pulse bandwidth is about two orders of magnitude higher than the Fourier transform limit for the given photon energy range. A conventional monochromator filter installed in the optical transport system could be used to narrow down the bandwidth of the FEL pulse, but in this way the filtering process would reduce the radiation energy by the same factor of 100. In contrast, self-seeding techniques [1, 2, 3] essentially filter the FEL radiation from a short part of the FEL setup to obtain a low-power, fully coherent seed, at a small delay of several tens of femtoseconds. The seed can overlap with the electron bunches delayed by a magnetic chicane that leads to generation of seeded FEL pulses which are subsequently amplified up to saturation (and beyond, by tapering) in the second part of the FEL undulator system. Build-up of two Hard X-ray Self-Seeding (HXRSS) installations as integrated devices is on-going at the SASE2 beamline of the European XFEL [4]. In this paper we report main features of HXRSS single crystal monochromator design.

Proceedings of the 13th International Conference on Synchrotron Radiation Instrumentation – SRI2018
AIP Conf. Proc. 2054, 030016-1–030016-6; https://doi.org/10.1063/1.5084579
Published by AIP Publishing. 978-0-7354-1782-3/$30.00

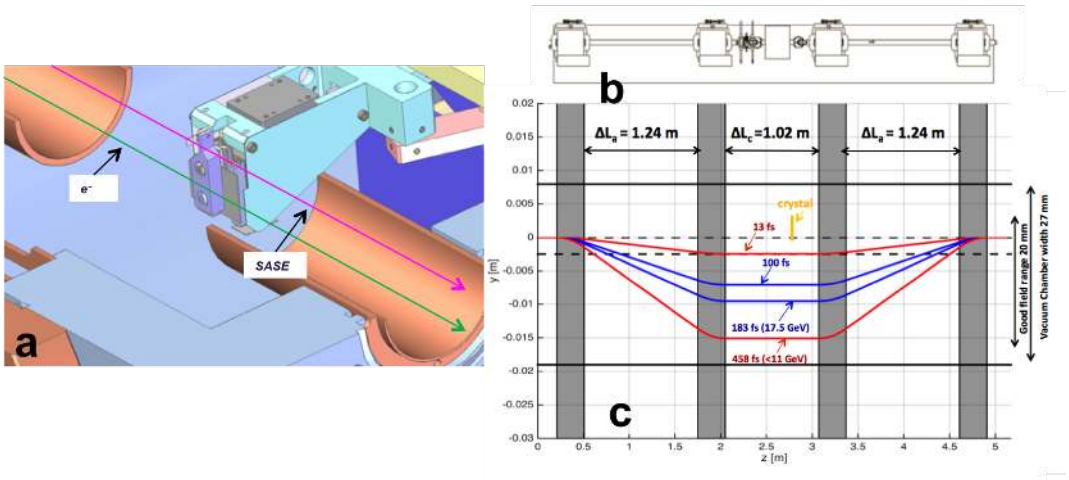

FIGURE 1. HXRSS chicane layout. a: SASE and e-beam trajectories inside the monochromator chamber; b: top view of the HXRSS chicane layout; c: chicane layout with electron beam trajectories inside the vacuum chamber. The yoke length is 0.3 m. Gray shaded boxes are the dipole magnets. A minimum distance of 2 mm is required from the edge of the crystal (in yellow) to the beam. Red lines represent the trajectories for the minimum offset of 2.5 mm (taking into account that the center of the defect-free area is 0.5 mm from the edge, Δt =13 fs) and maximum offset of 15 mm (Δt =458 fs). Blue lines are shown for the delay of 100 fs and for the maximum achievable delay of 183 fs at 17.5 GeV. Black lines show the width of the vacuum chambers, 37 mm.

MONOCHROMATOR DESIGN

The geometry of the monochromator is constrained from the side of the electron beam [5]. A minimum distance of 2 mm is required from the edge of the crystal to the electron beam. Therefore, the minimum beam offset is set to 2.5 mm to hit the crystal at 0.5 mm from its edge. In the Fig.1 one can see the trajectories for the minimum offset of 2.5 mm (Δt =13 fs) and maximum offset of 15 mm (Δt =458 fs for electron beam energy below 11 GeV)[1]. The flange-to-flange distance of the chamber in the beam direction is limited by 250 mm. The mechanical design of 4-axis positioning system shown in Fig.2b will be presented elsewhere. The base parameters of crystal positioning system are listed in Table 1 .

TABLE 1. Design specifications for European XFEL self-seeding monochromator

parameter	value	units
x position control range	-1.3 +9.7	mm
y position control range	±6	mm
crystal extraction position (approx)	x = +9.7	mm
crystal pitch angle operation range	30 - 120	deg
crystal tilt angle control range	-1 +4	deg
Vacuum	UHV	
Flange-to-flange distance with valves and bellows	255	mm

Diagnostics around the HXRSS monocromator chamber will consist of a camera and a screen capable of detecting the X-ray pulse reflected by the crystal (Fig.2 a and 3) to help in the first stages of commissioning of the HXRSS setups. The energy spectrum of the transmitted radiation will be measured using the single-shot spectrometer [9] in the experimental hutch and/or HIREX spectrometer in the photon tunnel [10].

[1] once the HXRSS crystals are retracted, such a large delay makes multiple-color experiments possible[6, 7, 8]

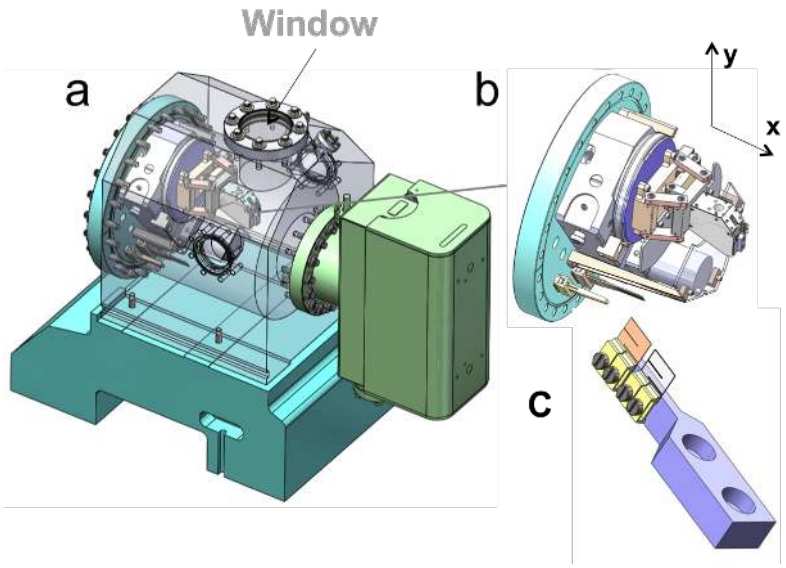

FIGURE 2. a) 3D model of monochromator vacuum vessel, window on the top has YAG screen inside, see also Fig.3; b) the flange with 4-axis positioning system; c) holder with two diamond single crystals; one can see two cuts on the right side of the crystal plates.

High Repetition Rate and Heat Load Mitigation

The European XFEL provides hard X-ray radiation of unprecedented quality in terms of peak brightness and short pulse duration [11, 12]. The electron bunch pattern is, unlike at storage ring facilities - very inhomogeneous in time, leading to a heat load of 10 kW or higher during the 600 μs long X-ray pulse train. At the SASE2 self-seeding layout this power will be concentrated on a spot with 0.035 mm diameter after seven undulator segments. The spontaneous radiation background absorbed in the crystal which can be estimated about 5.5 μ J per pulse in 0.5-300 keV photon energy range. Simulations results for the heat load distribution on a diamond monochromator crystal are shown in Fig.4. Simulations are done in 1D FEA approximation with no cooling (only transient part is taken into account), starting at 300K. 1000 pulses per train is considered as realistic target, with 220 ns spacing between pulses in the train. One can see that after 1000 pulses a temperature increase of 24 K is estimated (Fig.4 b). Meanwhile, the maximal crystal temperature increase that will preserve the Bragg angle inside the Darwin width can not exceed 11 K (FEL beam, 8K, see Fig.4 a). Therefore, a diamond monochromator with passive heat dissipation can be only used for shorter pulse trains and does not cover the whole operation range. A pitch oscillator, which can compensate, during the pulse train, the Bragg angle variation corresponding to up to 40K , is under development. Taking into account the diamond thermal expansion of 1.2 10^{-6} K^{-1}, the oscillator should provide angular velocities in the range 40 μrad per 0.2 ms.

Additional challenge is removing heat before arriving of the next pulse train. A holder of pyrolytic graphite used in LCLS design [13] would not be able to provide sufficient heat transfer. In the presented design the metal holders shown on Fig.2 c will be used instead, with two crystals clamped to one holder. To decouple the deformation causes by clamping from working area, special crystal shape was suggested by TISNCM. Two cuts (see Fig. 2 and 5) make it possible to get 'deformation-free clamping' and provide effective heat flow out of the radiated area. This approach was successfully tested with X-rays.

Diamond Crystals Characterization

The HTHP IIa type diamond plates for the monochromators have crystallographic orientations of 100, 111 and 110 with azimuthal orientations aligned along the main crystallographic directions. The plates have the thickness variation less than 5 μm, and misorientation less than 0.5 deg. The holders are made of vacuum and e-beam compatible materials, and should provide deformation-free mounting of the diamond crystal plates as discussed above, with maximal deformation of the top area 10^{-5}. All the plates are of size 5×5 mm, and one can observe the defect-free areas 1×1

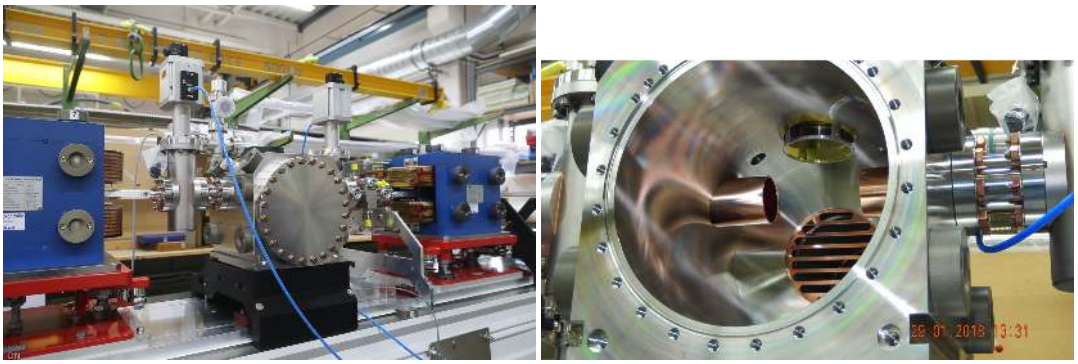

FIGURE 3. On the left: the girder with the HXRSS monochromator chamber and dipoles; on the right: monochromator chamber with YAG screen and HF shielding for ion getter pump.

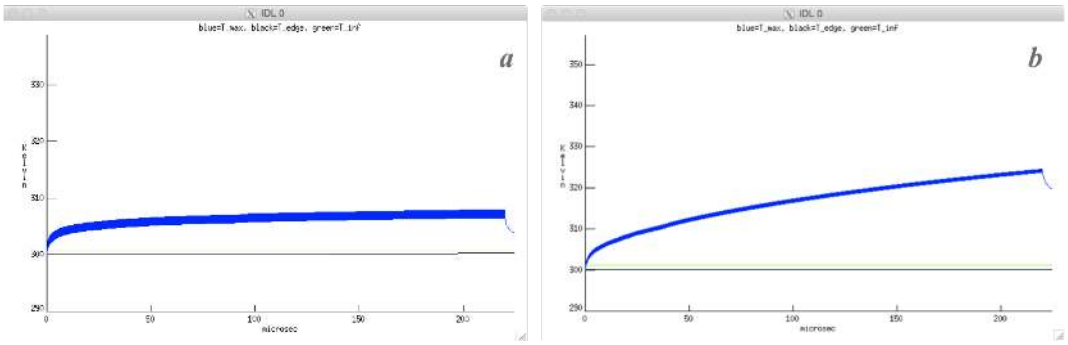

FIGURE 4. Heat load simulations (see text for details). a: FEL radiation without spontaneous component, simulation parameters: 1000 pulses, 3 μJ per pulse, 0.385 μJ absorbed, photon energy 8.3 keV, 0.1 mm thick diamond crystal, beam size 0.035 mm FWHM, $R_{crystal}$ 1 mm, T_{max} 308K; b: both, FEL and spontaneous radiation (SR) taken into account, simulation parameters: FEL beam size 0.035 mm , SR beam size 1 mm FWHM, absorbed power 0.385 + 5.5 μ J, $R_{crystal}$ 3 mm, T_{max}= 324K, absorbed power at 10 Hz: 0.58 W.

mm on the top of the plates on Figure 5. The full set of the crystals also includes more (100) 100 μm-thick diamond plates as well as several (111) diamonds of thicknesses between 35 and 55 μm, for operating at photon energies down to 3.5 keV.

CONCLUSIONS AND OUTLOOK

In conclusion, the design of diamond crystal hard X-ray self-seeding monochromator is presented. The main challenge for the monochromator is the high repetition rate of European XFEL source, the inhomogeneous pulse pattern, and a severe heat load on the monochromator crystal. For initial commissioning, no cooling will be used, which will put limitation on length and number of pulses used for self seeding. Two options, active cooling and installing a pitch oscillator for compensation of the temperature variation during the pulse train are considered for further development. By now the SASE2 chicanes, girders and monochromator chambers are assembled, the girders will be installed during the summer break. The full monochromator installation is scheduled for December 2018, and the commissioning is planned in the beginning of 2019. The HXRSS components for SASE1 should be ready for installation by the end of 2019.

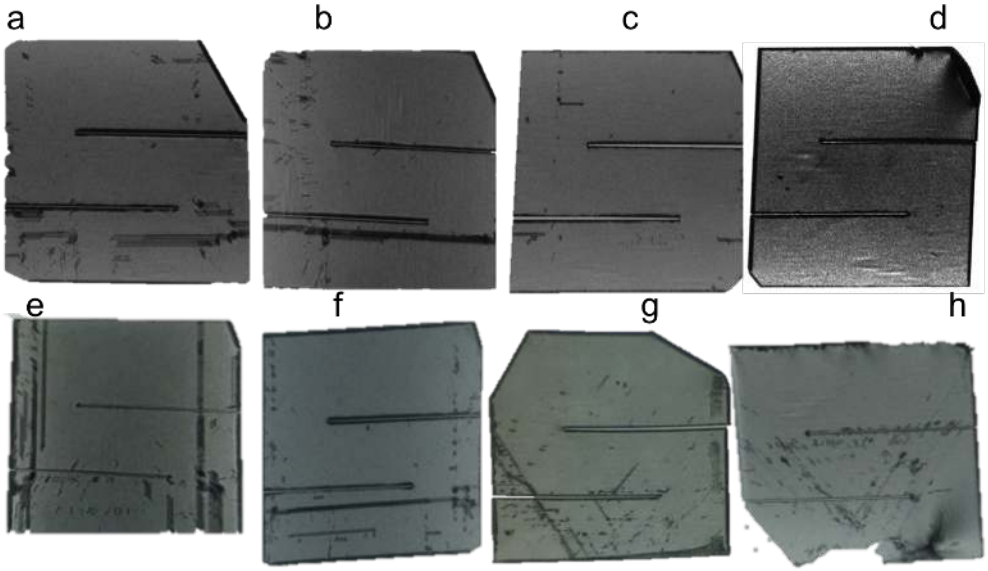

FIGURE 5. a) X-ray topograms of of 5×5mm HTHP IIa diamond crystal plates foreseen for the monochromator, a-f: (100) orientation, ; g: (111) orientation, thickness 100 μm; and h: (110) orientation. Most of the crystals have a thickness about 100 μm, except (a) and (e) which are of 160 μm.

ACKNOWLEDGMENTS

The presented work is done as a part of XFELSEED activity, a Russian-German project coordinated in the framework of the "Ioffe-Roentgen" cooperation (BMBF Verbundprojekt 05K2014 - XFELSEED). The work at Argonne National Laboratory is supported by the U.S. Department of Energy, Office of Science, under Contract No. DE-AC02-06CH11357 and Argonne WFO project 857Y2. We acknowledge the European Synchrotron Radiation Facility for provision of synchrotron radiation facilities and would like to thank Thu Nhi for assistance at the BM05 beamline.

REFERENCES

[1] J. Amann, W. Berg, V. Blank, F.-J. Decker, Y. Ding, P. Emma, Y. Feng, J. Frisch, D. Fritz, J. Hastings, Z. Huang, J. Krzywinski, R. Lindberg, H. Loos, A. Lutman, H.-D. Nuhn, D. Ratner, J. Rzepiela, D. Shu, Y. Shvyd'ko, S. Spampinati, S. Stoupin, S. Terentyev, E. Trakhtenberg, D. Walz, J. Welch, J. Wu, A. Zholents, and D. Zhu, Nature Photonics **6**, p. 693 (2012).

[2] G. Geloni, V. Kocharyan, and E. Saldin, Journal of Modern Optics **58(16)**, 1391–1403 (2011).

[3] T. Inagaki, T. Tanaka, N. Adumi, T. Hara, R. Kinjjo, H. Maesaka, M. Yabashi, H. Tanaka, T. Ishikawa, and H. Ohashi, Proc. FEL2014 Conference, Basel, Swizerland p. 603 (2014).

[4] X. Dong, G. Geloni, S. Karabekyan, L. Samoylova, S. Serkez, H. Sinn, K. Bernward, W. Decking, C. Engling, N. Golubeva, V. Kocharyan, S. Liu, A. Petrov, E. Saldin, T. Wohlenberg, D. Shu, V. Blank, and S. Terentiev, Proc. FEL 2017 Conference (2017), http://fel2017.jacow.de/papers/mop008.pdf.

[5] S. Liu, W. Decking, and L. Fröhlich, J. Phys.: Conf. Ser. **874**, p. 012022 (2017).

[6] G. Geloni, V. Kocharyan, and E. Saldin, 2010, preprint DESY 2010-004 available at https://arxiv.org/abs/1001.3510.

[7] T. Hara, Y. Inubushi, T. Katayama, T. Sato, H. Tanaka, T. Tanaka, T. Togashi, K. Togawa, K. Tono, M. Yabashi, and T. Ishikawa, Nat. Commun. **4:2919** (2013), doi: 10.1038/ncomms3919.

[8] A. A. Lutman, F.-J. Decker, J. Arthur, M. Chollet, Y. Feng, J. Hastings, Z. Huang, H. Lemke, H.-D. Nuhn, A. Marinelli, J. L. Turner, S. Wakatsuki, J. Welch, and D. Zhu, Phys. Rev. Lett. **113**, p. 254801 (2014).

[9] U. Boesenberg, L. Samoylova, T. Roth, D. Zhu, S. Terentyev, M. Vannoni, Y. Feng, T. B. van Driel, S. Song, V. Blank, H. Sinn, A. Robert, and A. Madsen, Optics Express **25**, 2852–2862 (2017).

[10] J. Gruenert, M. Planas Carbonell, F. Dietrich, W. Freund, A. Koch, N. Kujala, J. Laksman, J. Liu, and T. Maltezopoulos, This proceedings (2018).
[11] M. Altarelli and et al, Technical Report (2006), preprint DESY 2006-097.
[12] T. Limberg and W. Decking, Technical Note (2013), xFEL.EU TN-2013-004.
[13] D. Shu, Y. Shvyd'ko, J. Amann, P. Emma, S. Stoupin, and Quintana, J. Phys.: Conf. Ser. p. 603 (2013).